



**HAL**  
open science

# Nanostructuring lithium niobate substrates by focused ion beam milling

F. Lacour, N. Courjal, M.-P. Bernal, A. Sabac, C. Bainier, M. Spajer

► **To cite this version:**

F. Lacour, N. Courjal, M.-P. Bernal, A. Sabac, C. Bainier, et al. Nanostructuring lithium niobate substrates by focused ion beam milling. *Optical Materials*, 2005, 27, pp.1421-1425. 10.1016/j.optmat.2004.07.016 . hal-00095692

**HAL Id: hal-00095692**

**<https://hal.science/hal-00095692>**

Submitted on 27 Jan 2008

**HAL** is a multi-disciplinary open access archive for the deposit and dissemination of scientific research documents, whether they are published or not. The documents may come from teaching and research institutions in France or abroad, or from public or private research centers.

L'archive ouverte pluridisciplinaire **HAL**, est destinée au dépôt et à la diffusion de documents scientifiques de niveau recherche, publiés ou non, émanant des établissements d'enseignement et de recherche français ou étrangers, des laboratoires publics ou privés.

## Nanostructuring Lithium Niobate substrates by focused ion beam milling.

F. Lacour, M. Courjal, M.-P. Bernal,\* A. Sabac, C. Bainier, and M. Spajer

*Institut FEMTO-ST, Département d'Optique P. M. Duffieux,  
Université de Franche-Comté, UMR 6174 CNRS, 25030 Besançon cedex, France*

(Received 18 May 2004; accepted 14 July 2004)

We report on two novel ways for patterning Lithium Niobate (LN) at submicronic scale by means of focused ion beam (FIB) bombardment. The first method consists of direct FIB milling on  $LiNbO_3$  and the second one is a combination of FIB milling on a deposited metallic layer and subsequent RIE (Reactive Ion Etching) etching. FIB images show in both cases homogeneous structures with well reproduced periodicity. These methods open the way to the fabrication of photonic crystals on  $LiNbO_3$  substrates.

PACS numbers: 85.40.Ux ; 42.70.Qs ; 77.84.Dy

Keywords: Nano-structuring, Lithium Niobate, Focused Ion Beam, Reactive Ion Etching.

### I. INTRODUCTION

The recent development of integrated photonic crystals within planar waveguides can help implementing compact devices with fully integrable functions [1, 2, 3]. In these devices the light is confined into the crystal by a classical waveguide construction. Lithium Niobate (LN) is a suitable material for 2D photonic crystals because of its high refractive index. Moreover, its high electro-optic coefficient and its low optical losses make this material very adequate for optical communication systems. Therefore, the perspective of fabricating miniature electro-optical and all-optical LN devices is attracting the research on  $LiNbO_3$  nanostructuring [4, 5]. However, the obtention of good nanometric optical structures in  $LiNbO_3$  continues to be a difficult task due to its well-known resistivity towards standard machining techniques like wet etching [6].

In this paper, we report on two alternative methods based on focused ion beam (FIB) bombardment to produce photonic band gap structures on  $LiNbO_3$  substrates with a spatial resolution of  $70nm$ . The high resolution and the ability to drill holes directly from the sample surface make FIB milling one of the best candidates for designing good optical quality patterns at submicrometer scale [7]. The only constraint is that the sample surface

must be metallised and grounded to avoid charge accumulation. Firstly, we describe the method for directly etching the LN substrate by FIB milling through the metal. This method has been already employed to etch sub-micrometric one-dimensional structures in  $LiNbO_3$  [8]. The second related method is based on RIE etching after FIB milling of the metal layer which behaves as a mask. The advantage of this alternative solution is a lower exposure time. Another expected advantage would be a good replication of the mask shape in the whole hole depth. In both cases, the fabricated submicronic patterns are characterized by FIB imaging.

Before describing the two nanostructuring methods, we present the calculated conditions to obtain a photonic band gap for  $LiNbO_3$  substrates.

### II. NUMERICAL STUDY

Numerical calculations are carried out using the commercial software *BandSolve*. For a wavelength  $\lambda = 1.55\mu m$ , the ordinary and extraordinary indexes of the Z-cut  $LiNbO_3$  substrate are assumed to be  $n_o = 2.2151$  and  $n_e = 2.1410$ , respectively. According to our calculations, a 2D triangular lattice of holes can yield to a total TM photonic bandgap if the diameter  $D$  of the holes is larger than  $0.4p$ , where  $p$  is the triangular lattice period. The ratio  $D/p$  should be as large as possible in order to benefit from a large photonic band gap, but it cannot exceed 0.5 for technological reasons. Indeed, the walls between holes could collapse for diameters larger than  $0.5p$ . Fig.1 shows the band diagram obtained in

---

\*Electronic address: maria-pilar.bernal@univ-fcomte.fr; Website: <http://www.femto-st.fr/fr/Departements-de-recherche/OPTIQUE/>

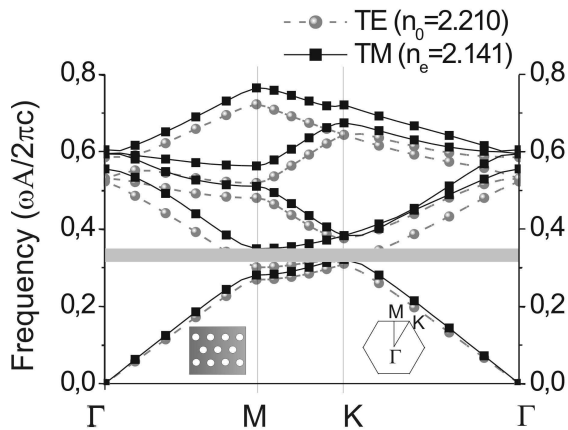


FIG. 1: TE and TM band structure for 2D triangular array.

the case  $D/p = 0.5$ . As it can be seen from the figure, the structure yields to a total TM-photonic band gap for frequencies between  $0.321p/(2\pi c)$  and  $0.349p/(2\pi c)$ . The difference from the calculation of S. Massy *et al.* [9] is probably the difference between the refractive index that are chosen in both cases. Having shown the existence of a photonic band gap in lithium niobate, we have investigated the means of nanostructuring it.

### III. EXPERIMENTAL

The two fabrication processes are schematically shown in Fig.2. The first method -Fig. 2(a)- is based on a direct etching of the  $LiNbO_3$  substrate by FIB milling. The second one -Fig. 2(b)- uses the FIB to create the metallic mask and the pattern is then transferred to the  $LiNbO_3$  substrate by RIE. In both cases the sample area is  $1cm^2$  and the thickness  $500\mu m$ . A  $Cr$  layer is deposited by electron gun evaporation (*Balzers B510*) and grounded with a conductive paste before introduction into the FIB vacuum chamber ( $= 2.10^{-6}torr$ ). In the case of direct FIB writing the thin  $Cr$  metal layer ( $150nm$ ) does not modify significantly the etching efficiency. In the second case a thicker  $Cr$  layer ( $250nm$ ) is deposited.

The metal-coated substrates are milled using a focused ion beam column *Orsay Physics LEO FIB4400* for the case of FIB milling only -Fig. 2(a)- and a *FEI Dual Beam Strata 235* for the milling of the metallic mask -Fig. 2(b). This method could be directly compared with e-beam lithography. The advantage of FIB patterning of the metallic mask is its ability to selectively remove and deposit material without the use of the additional process step of developing a resist layer.

In the first case (Fig. 2(a)) we have fabricated an array of  $4 \times 4$  circular holes with  $540nm$  diameter and  $1\mu m$  periodicity.  $Ga^+$  ions are emitted with a current of  $2\mu A$  and accelerated by a voltage of  $30kV$ . The ions are focused with electrostatic lenses on the sample with

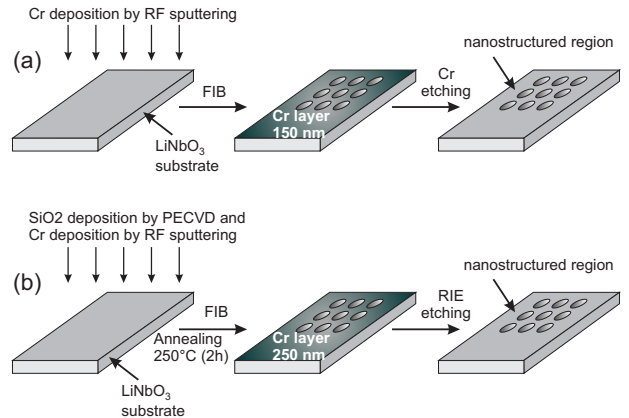


FIG. 2: TE and TM band structure for 2D triangular array.

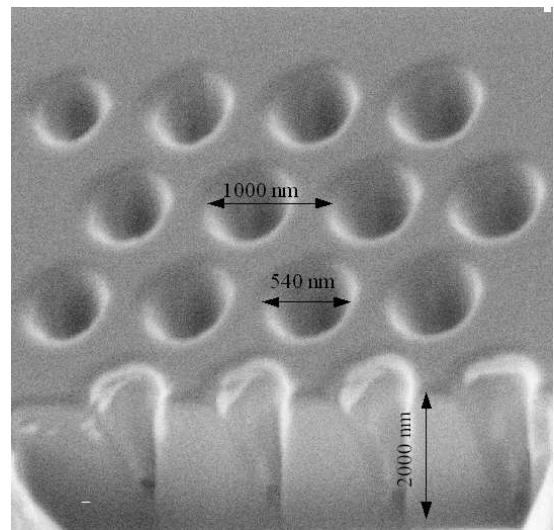


FIG. 3: FIB image of the FIB-etched  $LiNbO_3$   $4 \times 4$  array of circular holes.

a probe current of  $66pA$ . The pseudo-Gaussian-shaped spot size is estimated to be  $70nm$  on the target. The focused ion beam is scanned on the sample by a computer-controlled deflection field to produce the desired pattern (*Elphy Quantum* from *Raith*). A FIB-image cross-section of the cavities is shown in Fig. 3. In order to see the etching depth the sample is tilted  $30^\circ$  with respect to the FIB axis. As it can be seen from the image, the  $4 \times 4$  array exhibits well defined circular holes. The achieved etching depth is approximately  $2\mu m$  and the etching time was 12 minutes. At  $1\mu m$  deep the hole diameter is about  $432nm$ . This conical etching shape is due to material redeposition on the sidewalls while milling. In order to reduce the redeposition there are two possible solutions. If the FIB electronics is fast enough (*Elphy Quantum* is limited to  $300kHz$ ) and the spot size small enough one can scan along the hole sidewalls longer and less on the bottom of the pit. A second possibility that we plan to implement in our system is to use gas assisted milling. In particular,  $XeF_2$  could help to remove  $Nb$  from the

etched substrate decreasing then the redeposition.

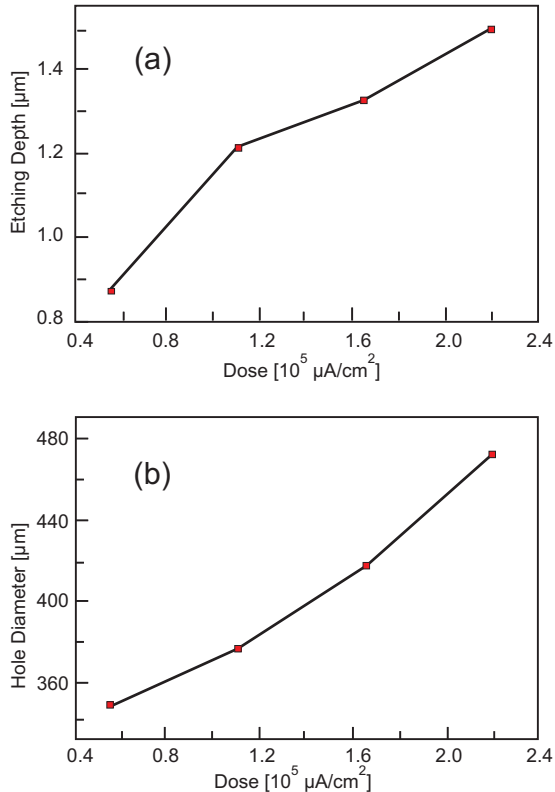


FIG. 4: (a) Dependence of the hole depth with respect to the  $\text{Ga}^+$  ion dose with a cross-section at the first hole-line plane. (b) Dependence of the hole diameter with respect to the  $\text{Ga}^+$  dose.

LiNbO <sub>3</sub>	Z-cut
Pressure	3mbar
SF <sub>6</sub> flow	10sccm
RF power	150W
Etching rate	50nm/min
LiNbO <sub>3</sub> /Cr selectivity	0.25

TABLE I: Parameters of the RIE process.

The etching depth and the real hole diameter can differ from the designed ones and this difference depends on the  $\text{Ga}^+$  dose. This can be clearly seen in Fig. 4 (a) and (b) where this dependence has been measured. It is clear from the graphs that as the milling time is increased, the etching depth increases but with a subsequent increase in the hole diameter due to beam aberrations. In particular, an increase of almost 30% in the hole diameter and of 40% in the etching depth has been measured as the  $\text{Ga}^+$  dose is increased by a factor of 4 from the initial value ( $4 \cdot 10^4 \mu\text{As}/\text{cm}^2$ ). Therefore, for practical uses one should start with a designed hole diameter slightly smaller than the desired one.

The second related process requires lower etching time since the desired photonic structure is fabricated at once. In this case, the FIB bombardment is used to pattern a  $\text{SiO}_2 - \text{Cr}$  mask previously deposited on the LN substrate, as depicted in Fig. 2(b). The first step consists in depositing a 100nm thick layer of  $\text{SiO}_2$  by Plasma Enhanced Chemical Vapor Deposition (PECVD). A 250nm thick chrome layer is then deposited on the substrate by sputtering. The metal is used as a mask for the RIE, while the silica layer prevents the diffusion of chrome into the substrate during the RIE plasma processing and the increase of the optical losses. This layer is not needed in the case of direct FIB milling since the etching is done locally and the damaged area is defined by the FIB beam size. The samples are annealed at  $250^\circ\text{C}$  during 2 hours to release stress. The  $\text{SiO}_2 - \text{Cr}$  mask is then nanostructured by FIB patterning, with a current of the sample of 100pA. An exposure time of 3.75s is typically required to etch a 250nm diameter circular hole, which is 11 times lower than the one required in the first process.

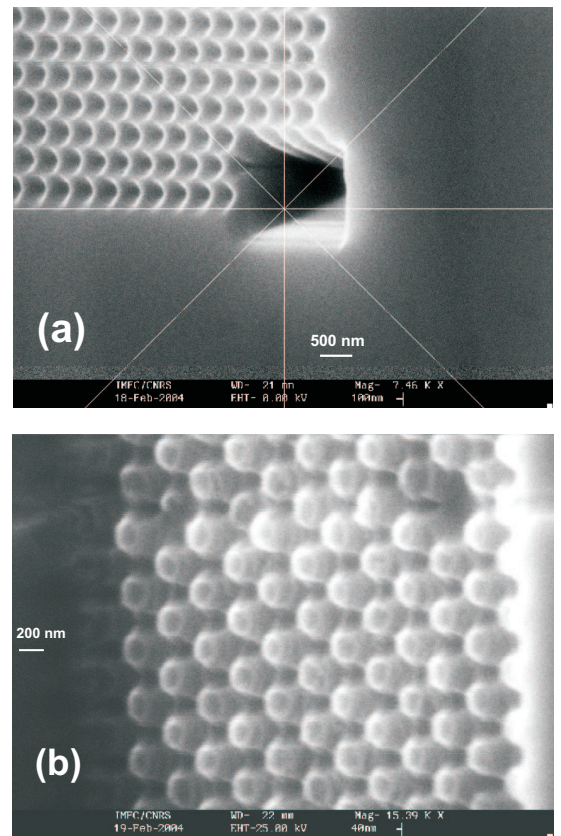


FIG. 5: SEM image of the  $\text{LiNbO}_3$  substrate covered by 250nm of Chrome after FIB milling and 10min of RIE etching. (a)  $D = 250\text{nm}$ , (b)  $D = 130\text{nm}$ .

The pattern (an array of  $24 \times 20$  cylindrical holes) is finally transferred to the substrate by RIE. The relevant parameters of this process are detailed in Table I. It can be noticed that this process requires a very low pressure and a high RF power. In these conditions, the etch

rate of the mask is comparable to the etching rate of the substrate. In order to improve the selectivity of etching between the mask and the  $LiNbO_3$  substrate, we start the process with an exposition of the target to a  $O_2$  ionic plasma (pressure =  $100\mu Bar$ , power =  $60W$ ). The  $250nm$  thick layer of chrome is then more resistant to the  $SF_6$  RIE. The selectivity of the mask is thus estimated to be 1 : 5 compared to the  $LiNbO_3$  substrate (while the etching selectivity was measured to be of 1 : 2 without the  $O_2$  ionic plasma). The etching rate of the Z-cut substrate is measured to be  $50nm/min$ . This process is applied to fabricate a triangular lattice of holes with  $D = 250nm$  and  $D = 130nm$  diameters and  $p = 2D$  periodicity. Fig. 5 (a) and (b) exhibit the SEM images of the holes after FIB milling and  $10min$  of RIE etching. Fig. 5(a) shows holes with good reproducibility. The etching depth is measured to be  $500nm$ . Fig. 5(b) shows that the  $130nm$  diameter holes were transformed into  $130nm$  diameter rods after RIE etching, while the  $250nm$  diameter holes were well preserved. This is due to a higher etching rate along the sides of the triangular lattice than in the triangle center when the holes are very close to each other. We can infer from these results that the fabrication of small holes ( $D \leq 200nm$ ) requires lower RF-power to preserve the initial feature.

#### IV. CONCLUSION

In this work we have presented two alternative techniques to fabricate submicrometric patterns in  $LiNbO_3$  by means of a FIB milling or a combination of FIB milling and RIE etching. In particular,  $500nm$ -diameter circular

holes were etched by FIB milling obtaining an etching depth of  $2\mu m$ . Material redeposition starts to be a problem for etching depths larger than  $1\mu m$ . A  $24 \times 20$  array of  $250nm$ -diameter circular holes and  $500nm$  periodicity was realized using an alternative method in which the metallic mask is fabricated by FIB milling and the  $LiNbO_3$  etching is obtained by  $SF_6$  RIE. In this case, the etching depth in  $LiNbO_3$  is around  $500nm$  and is limited by the metallic thickness of the mask. Work is in progress to optimize the RIE etching in view of obtaining a higher etching depth. An optical characterization of the patterns is also in progress.

As opposed to the process based on ferro-electric domain inversion, the presented methods are more suitable for implementing nanostructures on both X-cut and Z-cut substrates.

We are currently working on the theoretical analysis and the fabrication of active  $LiNbO_3$  2D photonic crystals. In order to operate at  $1.55\mu m$  our calculations show that we must have a triangular geometry of cylindrical holes of  $259nm$  diameter and  $519nm$  periodicity.

#### Acknowledgments

The authors want to thank Jacques Vendeville (FEMTO-ST, Université de Franche-Comté, Besançon) and Eloïse Devaux (Laboratoire des Nanostructures, ISIS, Université Louis Pasteur, Strasbourg) for technical assistance and Jean-Yves Rauch (FEMTO-ST, Université de Franche-Comté, Besançon) for fruitful discussions.

- 
- [1] M. Kamp, T. Happ, S. Mahnkopf, G. Duan, S. Anand and A. Forchel, *Physica E*, **21** (2004) 802.
  - [2] J. Zimmermann, M. Kamp, A. Forchel and R. Marz, Photonic crystal waveguide directional couplers as wavelength selective optical filters, *Optics Communication*, **230** (2004) 387.
  - [3] L. Wu, M. Mazilu, J. -F. Gallet and T. F. Krauss, Square lattice photonic-crystal collimator, *Photonics and Nanostructures - Fundamentals and Applications*, **1** (2003), 31.
  - [4] C. Restoin, S. Massy, C. Darraud-Taupiac and A. Barthelemy, Fabrication of 1D and 2D structures at submicrometer scale on lithium niobate by electron beam bombardment, *Optical Materials*, **22** (2003), 193.
  - [5] V. Foglietti, E. Cianci, D. Pezzeta, C. Sibilila, M. Marangoni, R. Osellame, R. Ramponi, Fabrication of Band gap structures in planar non linear waveguides for second harmonic generation, *Microelectronic engineering*, **67-68** (2003), 742.
  - [6] EMIS Data Reviews Series No. 5, Properties of Lithium Niobate (IN-SPEC, London and New York, 1989).
  - [7] C. G. Bostan, R.M. de Ridder, V.J. Gadgil, L. Kuipers, A. Driessen, Line-defect Waveguides in Hexagon-Hole type Photonic Crystal Slabs: Design and Fabrication using Focused Ion Beam Technology, *Proceedings Symposium IEE/LEOS Benelux Chapter, 2003, Enschede (The Netherlands)*.
  - [8] S. Yin, Lithium niobate fibers and waveguides: fabrication and application, *Proc. IEEE* **87**, (1999) 1962.
  - [9] S. Massy, C. Restoin, C. Darraud, and A. Barthelemy, Structures priodiques bidimensionnelles sur  $LiNbO_3$  et  $H_xLi_{1-x}NbO_3$  ralises par bombardement par faisceau d'lectrons, *JNOG 2003, Valence (France)*.